7 Defeitos Topológicos

Nesse capítulo vamos estudar os *defeitos topológicos*. Essa classe de defeito aparece em sistemas cuja fase é determinada pela quebra de uma simetria contínua.

Caracterização do defeito topológico: uma região - ponto ou linha - onde a ordem é destruída e um campo distante onde a variável elástica varia lentamente no espaço.

Exemplos:

- *vórtices* em modelos xy e no hélio superfluído
- *deslocamentos* em cristais periódicos
- *desclinações* em cristais líquidos nemáticos
- etc

Aplicações:

Fundamentais para determinar as propridedades dos sistemas reais, como por exemplo, as propriedades mecânicas de muitos materiais (rigidez).

Em duas dimensões eles são fundamentais para as transições de fase do sistema, adicionando rigidez ao sistema a baixas temperaturas (transições de fase de Kosterlitz-Thouless).

7.1 Caracterização dos defeitos topológicos

Modelo XY

$$< \vec{s}(\vec{r}) >= s(\cos\theta(\vec{r}), \sin\theta(\vec{r}))$$

função periódica em $\theta(\vec{r})$ $\rightarrow$é possível que $\langle \vec{s}(\vec{r}) \rangle$ seja contínua em todo lugar no espaço de dimensão-d exceto em um subespaço de dimensionalidade d_s menor que d. Exemplo para $d = 2$:

$$\theta(\vec{r}) = \phi + \theta_0$$

θ_0 é uma constante e $\vec{r} = (r, \phi)$. Então $\langle \vec{s}(\vec{r}) \rangle$ é contínua e $\vec{\nabla}\theta = 1/r$ é finito em todo lugar exceto na origem.

Na figura abaixo, $k = 1$ e $\theta_0 = 0, \pi/2, \pi$.

k=winding number (índice)=n

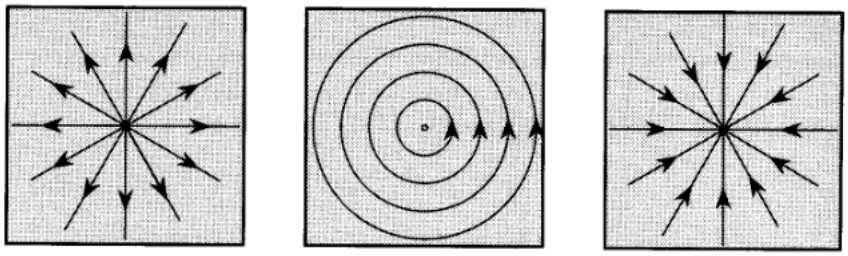

Figura 1: Confirgurações de vórtices com k=1: (a) $\theta = \phi$, (b) $\theta = \phi + \pi/2$, (c) $\theta = \phi + \pi$. (CL)

Podemos remover a singularidade na origem matematicamente (um ponto com dimensão $d_s = 0$). Para isso podemos cortar um buraco com raio ξ_0 ou fazendo o valor absoluto do parâmetro de ordem ir a zero na origem e ir ao seu valor de equilíbrio em um raio ξ_0 (ver figura abaixo).

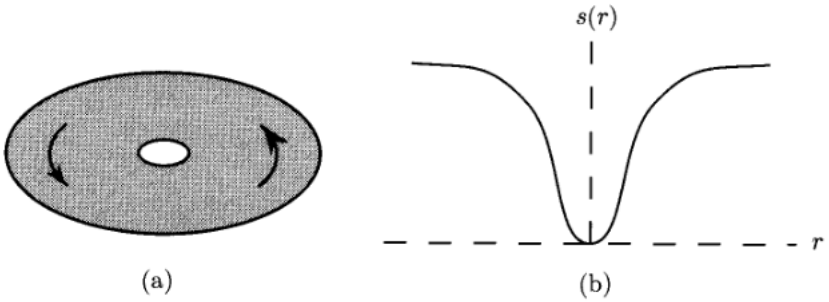

Figura 2: Remoção matemática da singularidade na origem (a) cortando um buraco e (b) reduzindo o valor absoluto do parâmetro de ordem para zero na origem e recuperando-o a uma distância da origem. (CL)

A configuração de spin, nesse caso denomina-se *vórtice*. O ângulo θ especifica a direção do parâmetro de ordem. Ele pode mudar por 2π em um circuito fechado, o qual engloba o vórtice na origem. Podemos sempre escrever

$$\begin{aligned} < \vec{s}(\theta) > &= \langle \vec{s}(\theta + 2k\pi) \rangle \\ k &= 0, \pm 1, \pm 2, ... \end{aligned}$$

Temos um número infinito de diferentes singularidas nas quais θ aumenta em $2k\pi$ em um circuito completo em torno da singularidade.

k (ou n) é denominada de *winding number* (número de enrolamento).

Para configurações de spin com valores pequenos de k podemos escrever

$$\theta(\vec{r}) = k\phi + \theta_0 \tag{1}$$

e a figura abaixo representa alguns casos.

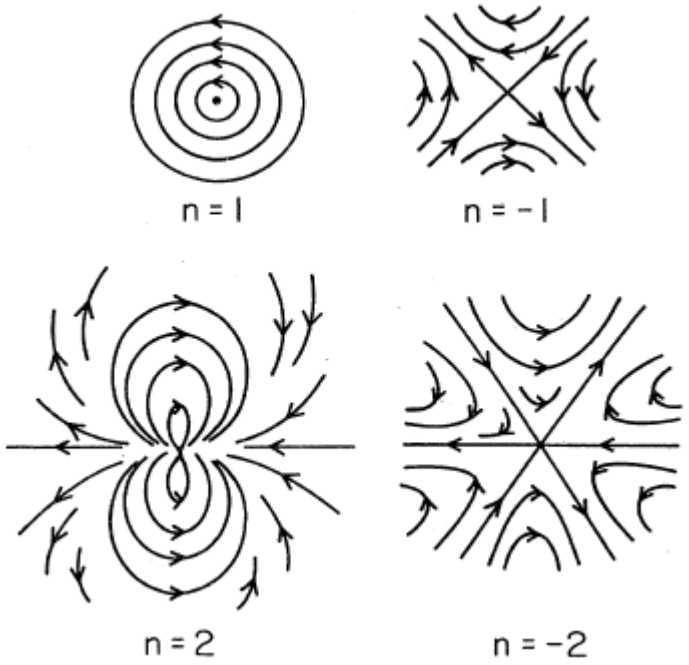

Figura 3: Singularidades pontuais de spins planares em duas dimensões com *winding number* igual a ± 1 e ± 2. (Mermin).

A existência de um inteiro não nulo para o *winding number* (índice de curva plana)implica necessariamente que há uma singularidade em $\vec{\nabla}\theta$ na origem. Podemos verificar isso facilmente: θ muda por $2k\pi$ em qualquer circuito em torno do núcleo (origem). Então, $\left|\vec{\nabla}\theta\right|$ no circuito a uma distância r do núcleo deve ser da ordem de $2k\pi/r$ e diverge com $r \to 0$.

It is important to mention that the physical variable $\langle\vec{s}(\vec{r})\rangle$, the order parameter, is perfectly continuous throughout the plane. It is only θ that undergoes a discontinuity. If $0 \leq \phi < 2\pi$ and θ obeys equation 1, then θ varies discontinuously by $-2k\pi$ as the positivie x-axis is traversed in a counterclockwise direction (we could as well define the opposite direction for the circle path). In that sense, the x-axis is a cut that introduces two imaginary surfaces (lines, in this case) along which θ has the values 0 and $2k\pi$ (see figure below). Observe that we can have different cuts as we choose different ranges of values for ϕ (for example, $-\pi \leq \phi < \pi$ instead of $0 \leq \phi < 2\pi$).

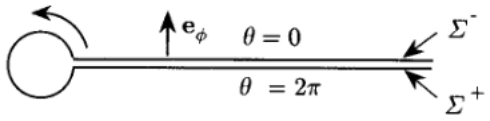

Figura 4: Cut accros which θ is discontinuous for the choice $0 \leq \phi < 2\pi$ of range values for ϕ. (CL)

The main characteristic of a *topological defect* is that it cannot disappear by any continuous deformation of the order parameter. We will analyse this with the example of the 2D vortex. Let us consider a distortion that is singularity free, as the one shown in fig. . It is easy to observe that we can perform a series of infinitesimal and continuous distortions and bring the system back to the order state.

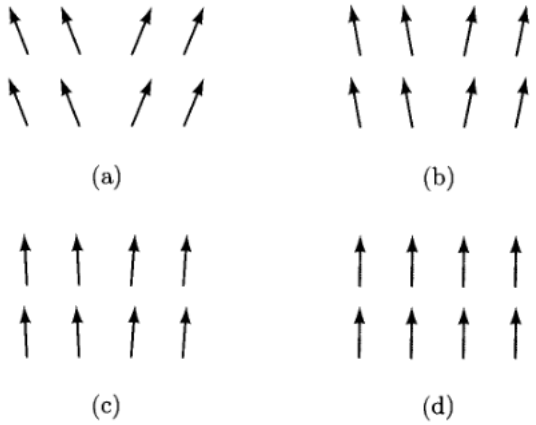

Figura 5: Sequence of distortions for a planar spin leading continuously to a distorted state singularity free to a state of total alignment. (CL)

Let us consider the case vortex $k = 1$, represented in the fig. (that is, $\theta = \phi + \pi$). Essentially, we cannot bring back this state to a perfectly aligned state by a sequence of infinitesimal continuous distortions of the order parameter. If we attempt to do so, the result is the one obtained in figure (b). To recover the total alignement we need to perform a series of discontinuous spin flips (change of the spin direction by a value of π). The energy of the state as shown in figure (b) is higher than the total alignment by a value of the order of JL where J i the exchange energy and L is the size of the sample. The initial configuration (in

(a)) has a lower energy, of the order of $J \ln L$. Therefore, it is unlikely that a fluctuation will destroy a single vortex. Another path to bring the vortex back to the total alignment would be to first take it back to the disorder state and then going to the uniform $\langle \vec{s}(\vec{r}) \rangle$. This process, however, will have an energy cost of the order of JL^2 and is even more unlikely to occur than the previous one. We can see that the vortex, although a state of higher energy, is a stable configuration. We say that the $k = 1$ vortex is a *topologically stable state*.

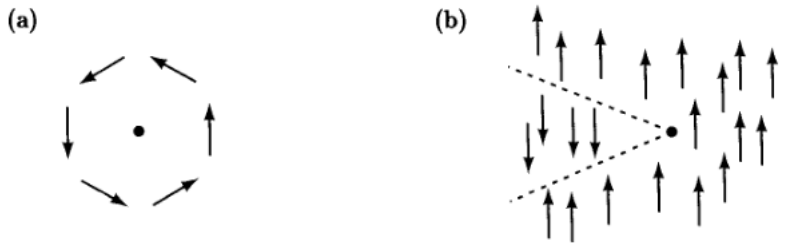

Figura 6: (a) $k = 1$ vortex. (b) Attempt to align the spins by a sequence of continuous distortions. (CL)

Actually, following similar arguments, it can be shown that we can only distort continuously a vortext with $k = 1$ to other configurations with the same value of k. There is an energy barrier to go from a state with one value of k to other with a differente value of k.

7.1.1 Vortex pairs

Let us consider here the case of pairs of vortices with opposite winding number and postpone the more general discussion for later on. Let us consider the case of figure . In this cse, it is easy to observe that far from the pair, the vectors $\langle \vec{s}(\vec{r}) \rangle$ are nearly parallel. We can approach the two vortices by continuous deformation and the region where the order parameter deviates significantly from the spatial uniformity decreases. Continuing this process, the two vortices will end up by annihilating each other. The pair of vortices with opposite values do not have an energy cost when compared to the perfectly aligned state. We will see later on that the winding number of pair of vortices just add. In this case, the vortex pair does not form a topologically stable state.

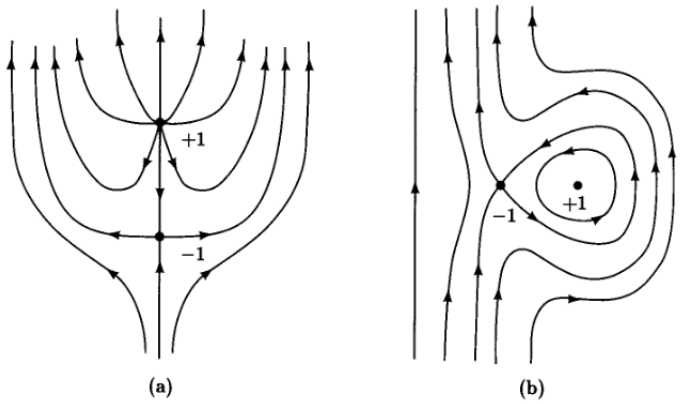

Figura 7: Vortex pairs of vortices with winding numbers equal to $k = 1$ and $k = -1$. (CL)

7.1.2 Order parameters with more than two components

Topological stability depens critically on the symmetry of the order parameter and its *codimension*. d is the dimension of the space. d_s is the dimension of the topological defect. n is the dimension of the order parameter. The codimension d' is defined as

$$d' = d - d_s$$

The case we consider until now, the dimensionality of the order paramenter and its codimension were both 2 since we were considering a point defect (vortex) which has $d_s = 0$.

We have stable topological defects in three dimensions if the defect is a line, with $d_s = 1$. In this case, $n = d' = 3 - 1 = 2$.

The generalization if that the vortex to a n-dimensional vector order parameter is stable if $d' = n$. As an example, we consider the *hedgehog* configuration with $d_s = 0$. In this case, $d' = 3$ and a three-dimensional spin in a three-dimensional space ($n = d' = 3$) is stable (see figure (a) below).

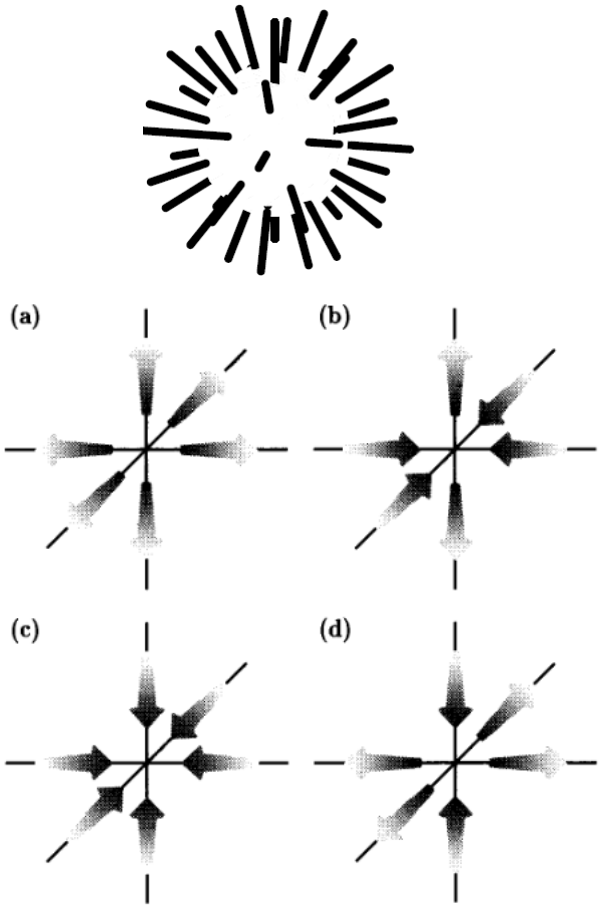

Figura 8: hedgehog; $\pi_2(S^2) = \mathcal{Z}$

In this case, we have an analog to the loop enclosing the vortex core. Here, we have a surface that encloses the center of the hedgehog. The same way, we have an index k characterizing the strength of the defect. Figure shows hedgehogs defects for $k = 1$ and $k = -1$. Observe that defects with the same value of k can be obtained one from the other by rotating $\langle \vec{s}(\vec{r}) \rangle$ by π along an axis.

Let us now consider the case when $n > d'$. In this case the topological defects are not stable. Let us consider, for example a three-dimensional spin system ($n = 3$) in a two-dimensional space. We can create a vortex configuration equivalent of a $k = 1$ vortex for two-component spins. Figure examplifies this situation. We can align the spins along the z-direction following the scheme shown in the figure which uses continuous infinitesimal changes

in the directions of the spins. The way to do that is taking advantage of the third dimension. As a consequence, a three-component spin a two-dimensional space is topologically unstable.

Finally, let us consider the case $n < d'$. In this situation it is simply impossible to construct configuration in which the order parameter rotates continuously around the core. One such example is the Ising model ($n = 1$) in two dimensions ($d = 2$). If we consider $s(\phi) = \cos\phi/\left|\cos\phi\right|$, then $s = +1$ for $0 \leq \phi < \pi$ and $s = -1$ for $\pi \leq \phi < 2\pi$. s changes discontinuously from -1 to 1 as we cross the x-axis. We have a line rather than a point defect. The ising model is a discrete symmetry and what we have is the formation of line defects and walls which are not the object of our study in this chapter.

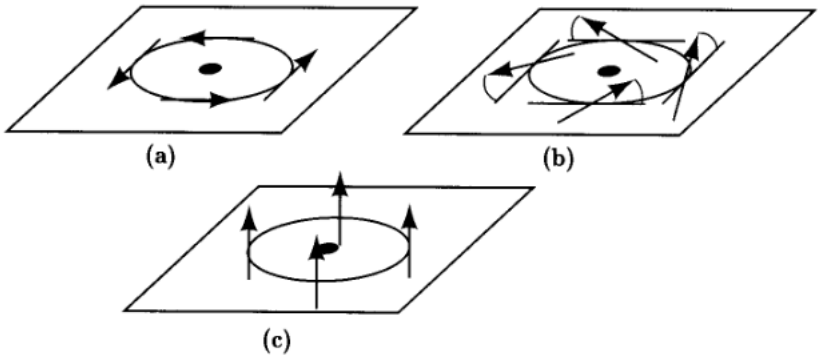

Figura 9: Sequence of distortions taking $n = 3$, $k = 1$ vortex state in two-dimension space into the aligned state. (CL)

7.2 Parâmetro de ordem e *espaço de parâmetro de ordem*

Os valores possíveis do parâmetro de ordem formam um espaço conhecido como *espaço do parâmetro de ordem.* A magnetização quebra a simetria rotacional do sistema e o parâmetro de ordem determina qual das direções foi "escolhida" nessa quebra de simetria. A magnetização pode ser uniforme em todo o sistema.

Podemos mapear o parâmetro de ordem definido em um espaço $\mathcal{D}$ em um espaço de parâmetro de ordem $\mathcal{M}$.

Espaço de parâmetro de ordem $\mathcal{M}$: é a "variedade do estado fundamental" (*ground state manifold*), i.e., o espaço de parâmetros que descreve mudanças no parâmetro de ordem que

não modifica a energia livre de equilíbrio .

parâmetro de ordem e espaço do parâmetro de ordem: especificar o parâmetro de ordem em algum domínio do espaço de coordenadas $\mathcal{D}$ define um mapeamento de $\mathcal{D}$ em $\mathcal{M}$.

Nosso interesse maior será no caso em que o parâmetro de ordem varia continuamente no sistema físico, exceto talvez em alguns pontos, linhas ou superfícies onde pode haver uma quebra da continuidade - diminuição da dimensionalidade - que são os *defeitos*.

Para entendermos melhor esses conceitos, vamos examinar alguns exemplos e como podemos expressar o parâmetro de ordem nesses casos.

Spins planares Consideremos um sistema físico bidimensional. Embora esse caso seja útil para exemplificar muitas situações, podemos encontrar sistemas onde essa situação ocorre, como filmes finos e outros sistemas físicos altamente anisotrópicos. A magnetização já está no sistema, a nível atômico ou molecular. A quebra da simetria ocorre pelo alinhamento dos spins dando origem a magnetização.

O parâmetro de ordem é um vetor de grandeza fixa (podendo ser igual a um por conveniência) forçado a ficar restrito a um plano. Podemos mapear esse parâmetro de ordem a uma circunferência. Para isso, vamos chamar $\vec{u}$ e $\vec{v}$ um par de vetores ortonormais no plano. Podemos escrever a função $f(\vec{r})$ na forma

$$f(\vec{r}) = m(\vec{r}) = \vec{u}\cos\varphi(\vec{r}) + \vec{v}\sin\varphi(\vec{r}) \tag{2}$$

$f(\vec{r})$ é a magnetização no plano. Podemos ver que o espaço do parâmetro de ordem (espaço euclidiano bidimensional, (x, y)) pode ser mapeado a circunferência de um círculo de raio fixo (unitário, em geral). Chamamos o novo espaço de $\mathcal{S}^1$.

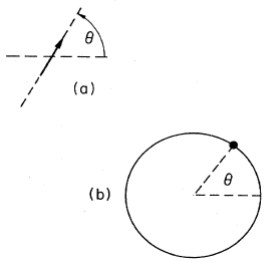

Figura 10: Representação no espaço de parâmetro de ordem.

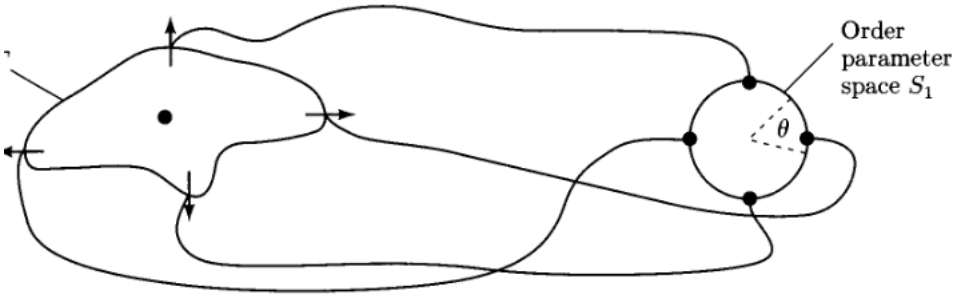

Figura 11: Representação do spin planar no espaço de parâmetro de ordem. (CL)

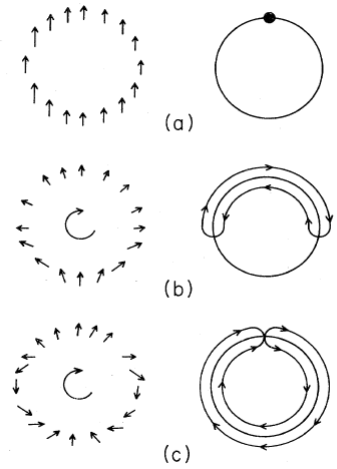

Figura 12: Configurações de spin em contornos circulares. (a) Fase ordenada. (b) Spin não uniforme com $n = 0$. (c) Spin não uniforme com $n = 2$. (ver Mermin).

Spins normais Esse é o caso dos spins tridimensionais. O parâmetro de ordem novamente é a magnetização $m(\vec{r})$ onde agora o espaço definido por $\vec{r}$ é o espaço tridimensional eu-

clidiano $\vec{r} \to (x, y, z)$. Podemos mapear esse espaço a uma esfera de raio fixo por meio da correspondência

$$\begin{aligned} f(\vec{r}) &= m(\vec{r}) = m_u(\vec{r})\vec{u} + m_v(\vec{r})\vec{v} + m_w(\vec{r})\vec{w} \\ &\text{onde } m_u^2 + m_v^2 + m_w^2 = 1 \end{aligned} \tag{3}$$

A figura mostra o mapeamento do parâmetro de ordem. Nesse caso, o espaço do novo parâmetro de ordem é $\mathcal{S}^2$.

É importante observar que nesses dois casos desprezamos a existência de um cristal quando o material magnético for um sólido cristalino. Isso significa que estamos tratando de ferromagnetos líquidos ou que podemos, em um certo nível de aproximação (longos comprimentos de onda) substituir a presença do campo cristalino por um meio contínuo.

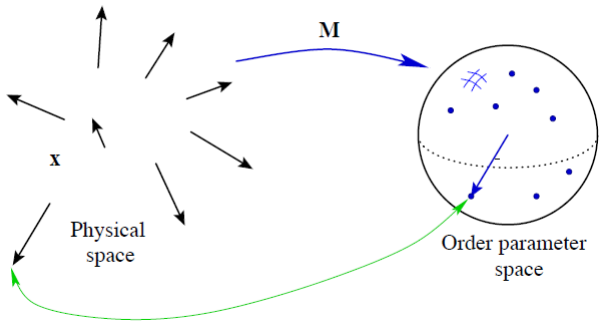

Figura 13: Parâmetro de ordem magnético projetado no espaço $\mathcal{S}^2$.

Cristais líquidos nemáticos Os cristais líquidos nemáticos apresentam uma quebra de simetria rotacional mas não translacional. Nesse caso o parâmetro de ordem descreve o eixo local de preferência no meio de moléculas relativamente longas (tipicamente dezenas de nanometros) com simetria aproximada de um elipsoide de revolução. A diferençã com a magnetização é que aqui não há direção preferencial, tanto faz alinhar-se na direção "norte" ou "sul". O parâmetro de ordem é um vetor "sem ponta", $\vec{n} = -\vec{n}$. Vamos utilizar esse

exemplo para discutirmos mais de uma possibilidade para representar o parâmetro de ordem (o que normalmente é o caso).

- A primeira possibilidade, seguindo os exemplos anteriores, é considerarmos a projeção do vetor $\vec{n}$ em uma esfera. Nesse caso, no entanto, é suficiente que façamos a projeção em apenas um hemisfério uma vez que uma rotação de π deixa o vetor invariante. A figura mostra esse caso. O resultado é que o caminho exemplificado na figura é um *caminho fechado* uma vez que os pontos no equador são equivalentes. Esse espaço é conhecido como *plano projetivo* $\mathcal{P}_2$ *(projective plane) ou* $\mathcal{RP}_2$. Sem entrar em detalhes, significa que o espaço deve ser visto como uma superfície em uma esfera normal tridimensional, com a identificação apropriada dos pares de pontos, da mesma forma que um círculo pode ser visto como um segmento de linha com os pontos terminais identificados.

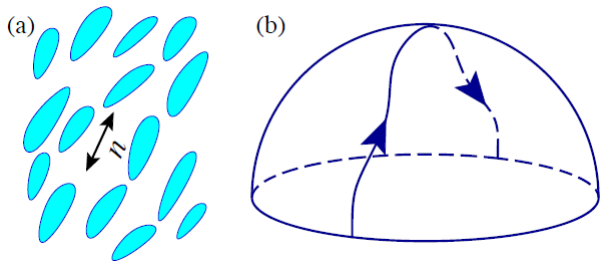

Figura 14: (a) Cristal líquido nemático esquematicado, mostrando o vetor $\vec{n}$, que é o parâmetro de ordem. (b) Projeção do espaço do parâmetro de ordem no hemisfério. O caminho representado é um caminho fechado nesse espaço uma vez que os pontos de partida e chegada são equivalentes. Extraído de .

- Uma outra forma de representar o parâmetro de ordem, que evita a falta de direção do vetor $\vec{n}$, é a diádica

$$f(\vec{r}) = M(\vec{r}) = \hat{n}(\vec{r})\hat{n}(\vec{r}), \ (M_{ij} = n_i n_j) \tag{4}$$

M é o operador projeção de $\vec{n}$ e quando especificamos M damos toda a informação

sobre $\vec{n}$ exceto pelo sinal de sua direção (que justamente é irrelevante).

- Podemos ainda subtrair de M uma constante multiplicada pelo tensor unitário o que produz uma matriz real simétrica e sem traço com um par de autovalores degenerados. Essa é provavelmente a forma mais física (concordas?) de representar o parâmetro de ordem. Ele pode ser visto como um desvio da isotropia de qualquer propriedade tensorial do meio.

Cristal Em um cristal, há a quebra da simetria translacional, substituída pelo arranjo periódico de sua célula unitária. Para cada cristal também está associado um grupo de simetria. Vamos considerar o caso simples de um cristal bidimensional que se cristaliza (configuração de mais baixa energia) em uma rede quadrada. Vamos considerar também a quebra dessa simetria pelo deslocamento (pequeno) dos seus átomos em relação a sua posição de equilíbrio. Vamos identificar esse deslocamento por $\vec{u}(\vec{r})$. A figura exemplifica essa situação.

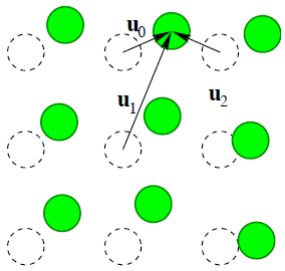

Figura 15: Cristal bidimensional em uma rede quadrada mostrando o campo vetorial dos deslocamentos $\vec{u}(\vec{r})$ em relação a posição de equilíbrio dos átomos. Extraído de .

O parâmetro de ordem $\vec{u}(\vec{r})$ não é exatamente um vetor. Como podemos ver pela figura, há sempre uma ambiguidade em relação a qual átomo ideal (da rede não perturbada) estamos nos referindo para o deslocamento. O vetor de deslocamento $\vec{u}$ muda por um múltiplo da constante de rede sempre que mudamos o átomo de referência:

$$\vec{u} \equiv \vec{u} + a\hat{x} \equiv \vec{u} + ma\hat{x} + na\hat{y} \tag{5}$$

O conjunto de parâmetros de ordem diferentes formam um quadrado com condições periódicas de contorno (ver fig.), o qual possui a mesma topologia que um torus $\mathcal{T}^2$.

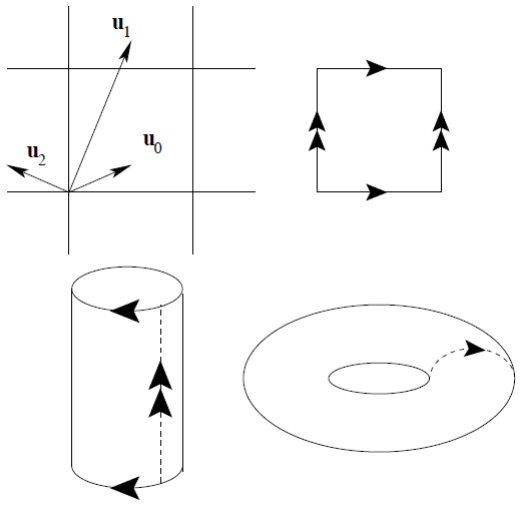

Figura 16: Espaço do parâmetro de ordem dos dislocamentos atômicos em uma rede quadrada. Extraído de .

Helio superfluido-4 Vamos mencionar esse exemplo para ilustrar sistemas com parâmetro de ordem mais complexo. Nesse caso, o parâmetro de ordem é uma função complexa $\Psi(\vec{r})$ que representa a função de onda do condensado, ou seja, o estado quântico único, fundamental, ocupado por uma considerável (macroscópica) fração de pares de Cooper ou pares de átomos do helio. A quebra de simetria está relacionada ao número de átomos. No estado normal, o número de átomos é conservado. No helio superfluido, o número de átomos é indeterminado (estão condensados na função de onda delocalizada). Podemos escrever o parâmetro de ordem na forma

$$\Psi(\vec{r}) = |\Psi(\vec{r})| \exp(iS(\vec{r})) \tag{6}$$

A magnitude da função de onda é fixada pela temperatura e o parâmetro de ordem é determinado pela fase, ou seja, pelo número complexo de magnitude $|\Psi|$. O parâmetro de ordem pode, portanto, ser projetado em um círculo $\mathcal{S}^1$. A formação do estado superfluido é

uma manifestação da quebra da simetria de calibre. Lembremos que a invariância de calibre do campo eletromagnético traduz-se na mecânica quântica por uma invariância da fase global. Efetivamente, se fazemos uma transformação $\vec{A} \to \vec{A} + \nabla\varphi$ no campo eletromagnético, temos uma mudança de fase da função de onda. A formação do estado superfluido (e similares) implica na impossibilidade do estado coletivo poder mudar de fase ou seja ele fica com uma fase coletiva bem definida, quebrando a simetria invariância por calibre. Não está no escopo desse curso discutir esse caso e nos limitaremos apenas a essa descrição qualitativa.

Apenas para mencionar, o helio superfluido-3 é bem mais complexo e possui várias fases, com vários regimes em cada fase. Não discutiremos esse caso (ver ref.).

A discussão acima mostra alguns exemplos de parâmetro de ordem e nos ajuda a entendermos o conceito. Também exemplificamos como podemos apresentar o espaço do parâmetro de ordem (também conhecido por *variedade dos estados internos - "manifold of internal states"*) de diferentes formas. Em particular, enfatizamos a apresentação do parâmetro de ordem na forma de *parâmetro de ordem topológico.* Essa representação facilita a discussão posterior, em particular na questão de defeitos.

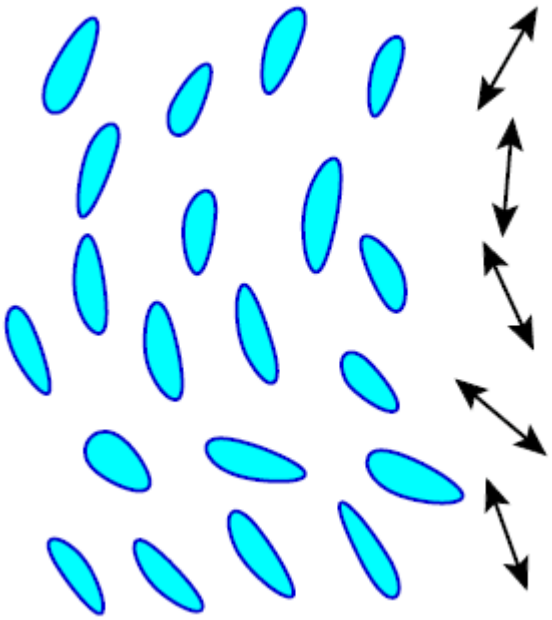

Figura 17: Onda rotacional em cristais líquidos nemáticos.

7.3 Homotopia

Homotopia: dois mapas f_0 e f_1 são definidos *homotópicos* se eles podem ser continuamente deformados um no outro, i.e., se existe uma família de mapas de um parâmetro h_t tal que $h_{t=0} = f_0$ e $h_{t=1} = f_1$. A construção explícita da deformação de $f_0$em f_1 é chamada de *homotopia.*

Classes de homotopia: defeitos estão na mesma classe de homotopia se os mapas de todos os caminhos englobando-os pode ser continuamente deformado um no outro. No modelo xy bidimensional as classes de homotopia dos defeitos pontuais são os índices do número de vezes que o caminho contorna $\mathcal{S}_1$, isto é o índice k (*winding number*).

Consideremos agora o exemplo do modelo O_3, com os loops mapeando o espaço do parâmetro de ordem S_2. Eles são todos homotópicos uma vez ue qualquer caminho fechado na superfície da esfera pode ser deslizado até o polo (ver figura). Temos apenas uma única classe de homotopia. Essa é a situação descrita anteriormente do spin de três dimensões em um espaço bidimensional.

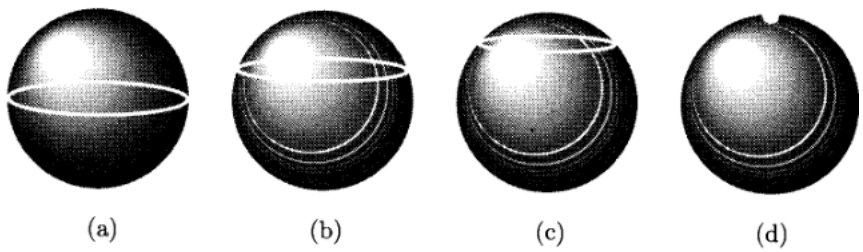

Figura 18: Continuous distortion of $n = 3$ vortex (line around equator of S_2) to the aligned state (point at a pole of S_2). (CL)

Grupo de homotopia fundamental ou primeiro grupo e homotopia de $\mathcal{M}$ é o grupo de caminhos fechados no espaço de parâmetros $\mathcal{M}$, $\pi_n(\mathcal{M})$, onde n é a dimensão da superfície esférica. Para o modelo xy bidimensional, $\pi_1(\mathcal{S}_1) = \mathcal{Z}$, onde $\mathcal{Z}$ são os números inteiros.

Grupo de homotopia zero: grupo que classifica as paredes de domínios

Primeiro grupo de homotopia:

Segundo grupo de homotopia: o defeito é envolvido por uma esfera bidimensional

Terceiro grupo de homotopia: defeitos em materais tri-dimensionais, texturas em matéria condensada e skyrmions em teoria de partículas

Quarto grupo de homotopia: defeitos integrais de caminho no espaço-tempo, também chamados de *instantons*.

The real value of the homotopy theory is to provide a natural group structure for combining effects. We already discussed this situation in the presence of two vortices that annihilated each other. Let us generalize this situation. Essentially, The topological defects are associated with homotopy classes of the order parameter space. The rules for combining defects are equivalent to rules for combining paths in different homotopy classes in the order parameter space. Let us consider the first homotopy group, $\pi_n(\mathcal{M})$. Consider two vortices as depicted in fig. , with winding numbers k_1 and k_2 located at different points in space. It is easy to show that the path enclosing both vortices is homotopic to the two paths enclosing the vortices individually. This happens because the change in θ in going from A to B is exactly equivalent but negative to the change in going from C to D, cancelling each other. In this case, the rule to combine vortices is just add their winding numbers. The group is simply Z, that is, the group of integers under addition, and we write as $\pi_1(S_1) = Z$. In general, we can write

$$\pi_n(S_n) = Z$$

This means that there are topologically stable configurations indexed by an integer for $n+1$ dimensional spins in an $n+1$ dimensional space for all $n \geq 1$.

Figure gives an example of this situation, where we show two topologically equivalent defects.

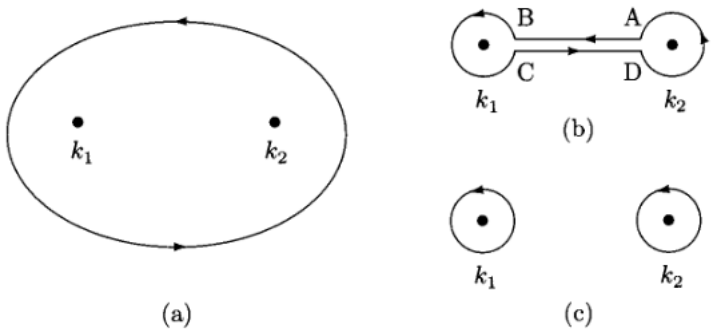

Figura 19: Sequence of distortions taking a loop around two vortices $k_1$and $k_2$to two loops around the individual vortices. (CL)

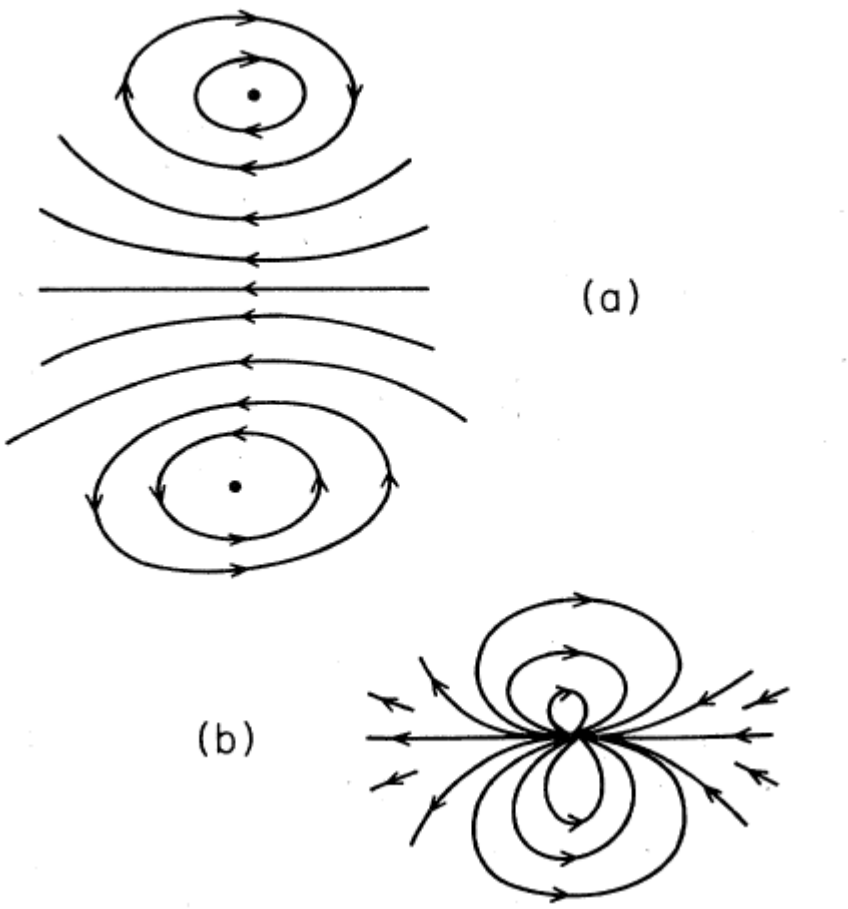

Figura 20: Two planar spin defects with winding number $k = +1$ and the topologically equivalent single planar spin defect with winding number $k = +2$. (Mermin)

Let us now consider the case of all configurations of three-dimensional spins in $d = 2$,

remembering that they are all homotopic. Therefore, $\pi_1(S_2)$ is the equivalent group consisting only of the identity element. We have then $\pi_1(S_2) = 0$. In general,

$$\pi_n(S_m) = 0, \;\; m > n$$

7.4 Examples of topological defects

7.4.1 Vortices in xy model

This is the case we have been mostly discussing so far. The defects are characterize by a mapping from some loop Γ in real space onto the order parameter space. The physical order parameter remains single-valued in a complete circuit of Γ (see fig.). We have then,

$$\oint d\theta = \oint_\Gamma \frac{d\theta}{ds} ds = 2\pi k, \;\; k = 0, \pm 1, ..., s$$

In two dimensions, the core is a point while in three dimensions it is a line (see fig.).

Free standing smectic-C filmes allow the observation of the vortices. Interference effects in the polarization light show clearly the existence of the vortices. See Van Winklew and Clark, Phys. Rev. A **38**, 1573 (1988)).

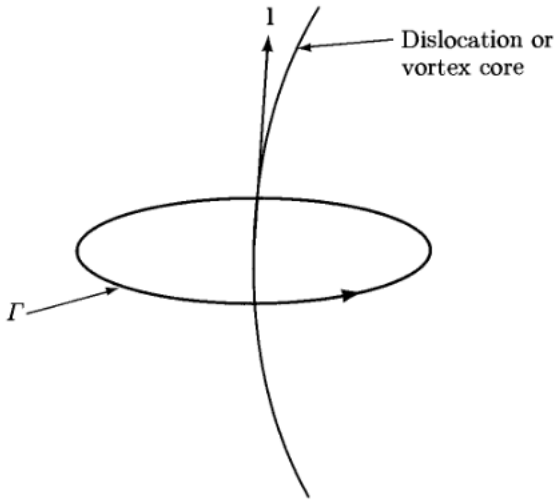

Figura 21: Loop Γenclosing a defect core with tangent vector $\vec{l}$. (CL)

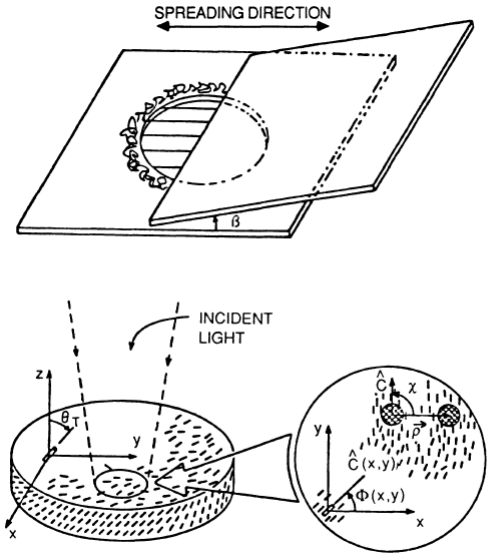

Figura 22: Schematic representation of a free standing smectic-C film.

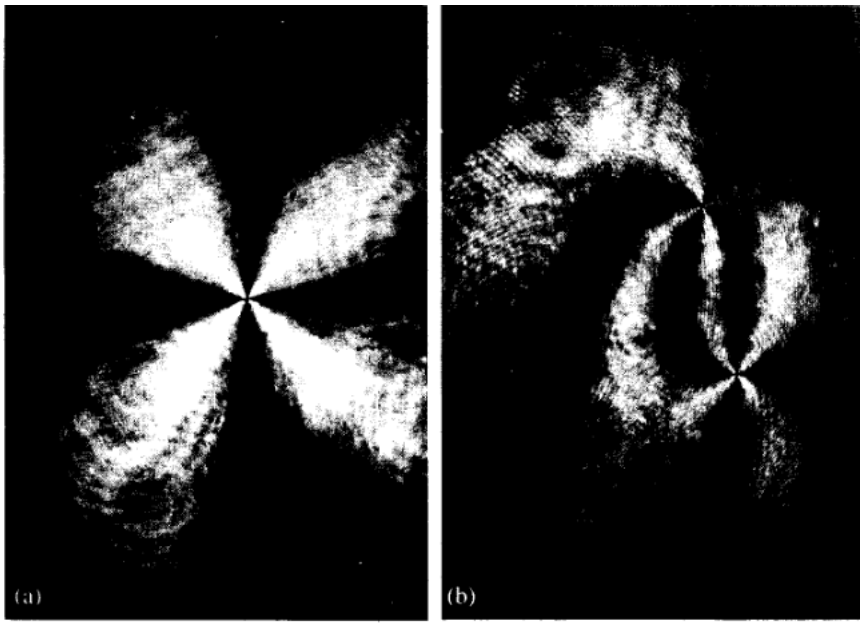

Figura 23: (a) Single unit and (b) disclination pair in a free standing smectic-C film. (CL)

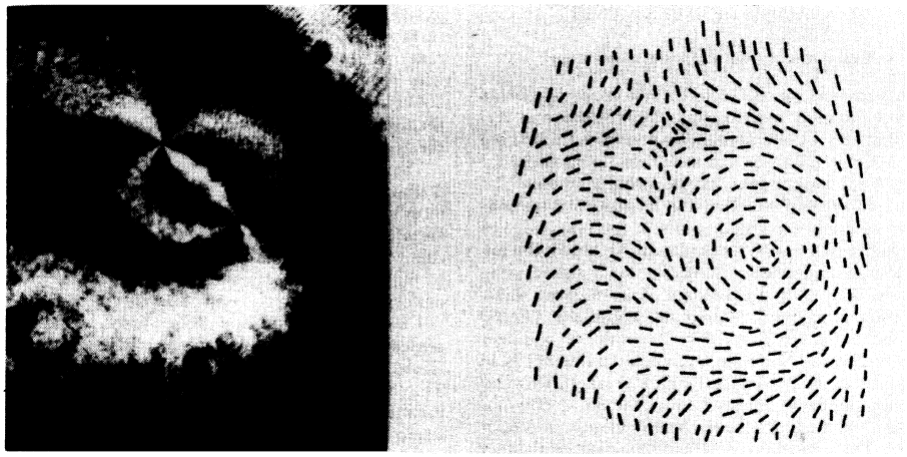

Figura 24: ± 1 disclination pair of FSLCF of racemic DOBAMBC in its SmC phase.

7.4.2 Periodic solids

As we already discussed, the elastic variable analogous to θ in a periodic solid is the vector displacement field $\vec{u}(\vec{r})$. A topological defect here is a dislocation, as it is shown in figure .

Figure shows how to represent the defect in the order parameter space represented by a torus $\mathcal{T}^2$. We consider a closed loop around the defect. The order parameter field $\vec{u}$ changes

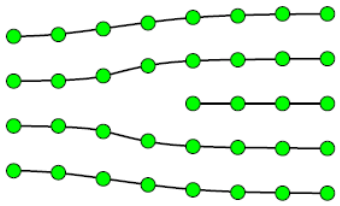

Figura 25: Dislocation in a crystal. (Sethna)

as we move around the loop. The positions of the atoms around the loop with respect to their local "ideal" lattice drifts upward continuously as we traverse the loop. This precisely corresponds to a loop around the order parameter space: the loop passes once throgh the hole in the torus. A loop around the hole corresponds to an extra column of atoms. Two loops which traverse the torus the same number of times through and around are equivalent. The equivalence classes are labelled precisely by pairs of integers (as we will discuss soon, just like the Burger's vectors), and the first homotopy group of the torus is $Z \times Z$.

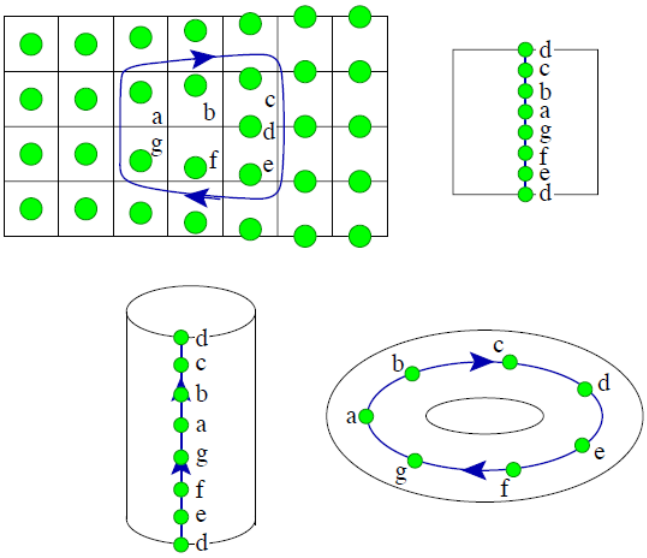

Figura 26: Loop around the dislocation mapped onto order parameter space for a 2D crystal. (Sethna)

We characterize the dislocation by

$$\oint d\vec{u} = \oint_{\Gamma} \frac{d\vec{u}}{ds} ds = \vec{R} = \vec{b}$$

where Γ is a curve enclosing the defect. This equation defines the mapping depicted in the figure below: a curve from the origin to $\vec{b}$ in the order parameter space is traced out as the core is encircld along Γ. The set of vectors $\vec{R}$ indexing the strength of the dislocations are the Burgers vectors $\vec{b}$ of the crystal. In periodic crystals, the Burgers vector lattice and the direct lattice of atomic positions are equivalent.

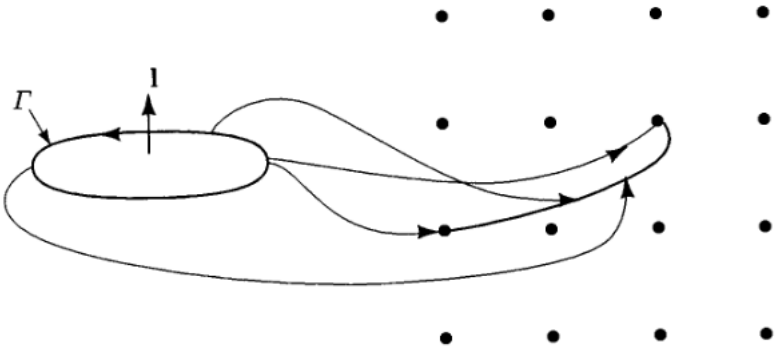

Figura 27: Two-dimensional Burgers vector lattice and mapping of a loop Γ onto a path between Burgers vectors in the order parameter space. (CL)

We can determine the Burgers vector of a dislocation in asimple manner. For that consider fig. . We go around any closed path in an ideal crystal following nearest neighbor bonds in the lattice. We count the number of steps along nearest neighbor bonds that are made in each of the lattice directions in completing the circuit along this path. We then follow exactly the same sequence of steps in a path around a dislocation core satrting at a point S and ending at a point E. This path is not closed. The vector from S to E is the Burgers vector characterizing the strength of the dislocation.

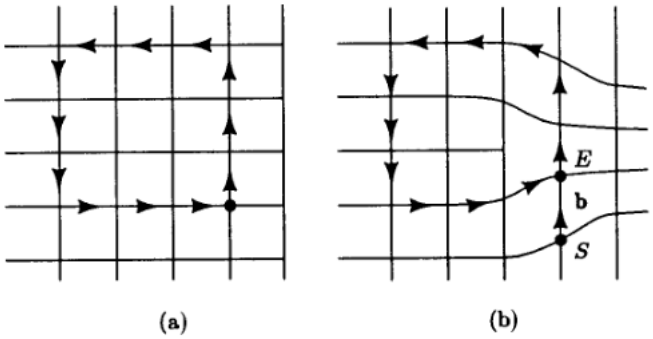

Figura 28: Burgers vector circuit in an undislocated (a) and a dislocated lattice (b). The Burgrs vctor $\vec{b}$ is the vector SE. (CL)

We can now characterize the defects in a 2D square crystal. We have two integers, the number of time we go around the central hole, and the number of times we pass through it. In the traditional, this corresponds exactly to the number of extra rows and columns of atoms we pass by. This is the Burger's vector and we identify now with the homotopy group of the torus,

$$\pi_1(\mathcal{T}^2) = Z \times Z$$

where Z are integers. The defect is indexed by two integers (m, n) where m represents the number of extra rows of atoms on the right-hand part of the loop and n represents the number of extra columns of atoms of the bottom.

7.4.3 Hedgehog in magnets

Figure shows a hedgehog defect for a magnetic system. The magnetization points straight out, and is given by

$$\vec{M}(\vec{r}) = M_0 \frac{\vec{r}}{r}$$

In this case, as we already discussed, we surround the sphere by a closed surface. As

we move around the sphere in ordinary space, the order parameter moves around the order parameter space which is also a spher of radius $M_0 = \left|\vec{M}\right|$. The order parameter space is covered exactly once as we surround the defect. This is called the *wrapping number*. As in all other cases of topological defects, it does not chance as we change the magnetization in smooth ways. The point defects are classified by the wrapping number:

$$\pi_2(S^2) = Z$$

The subscript 2 indicates that we are in the second homotopy group, that is, we are surrounding the defec with a 2D spherical surface.

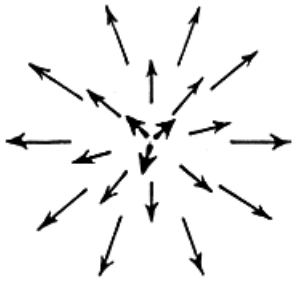

Figura 29: Hedgehog for magnetic systems. (Sethna)

7.4.4 Nematic defects

In this case, we do not have any difference related to the orientation of the molecule. For the two dimensional nematic we have invariance for $\vec{n} \to -\vec{n}$. The order parameter space isthe unit circle with opposite points identified (i.e. $\theta = 0$ and $\theta = \pi$ are equivalent). This space is denoted by $\mathcal{RP}^1$, denoting the projective space of one-dimension. We have a topological stable defect if we satisfy the condition

$$\oint_\Gamma \frac{d\theta}{ds} ds = \pm\pi$$

Disclinations with tangent lines for $k = \pm 1/2$ are shown in fig. . We can also have

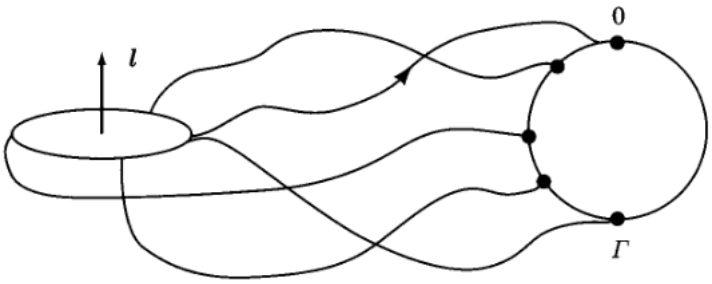

Figura 30: Mapping betwen the circuit Γ and the orde parameter space for a +1/2 disclination i na two-dimensional nematic. (CL)

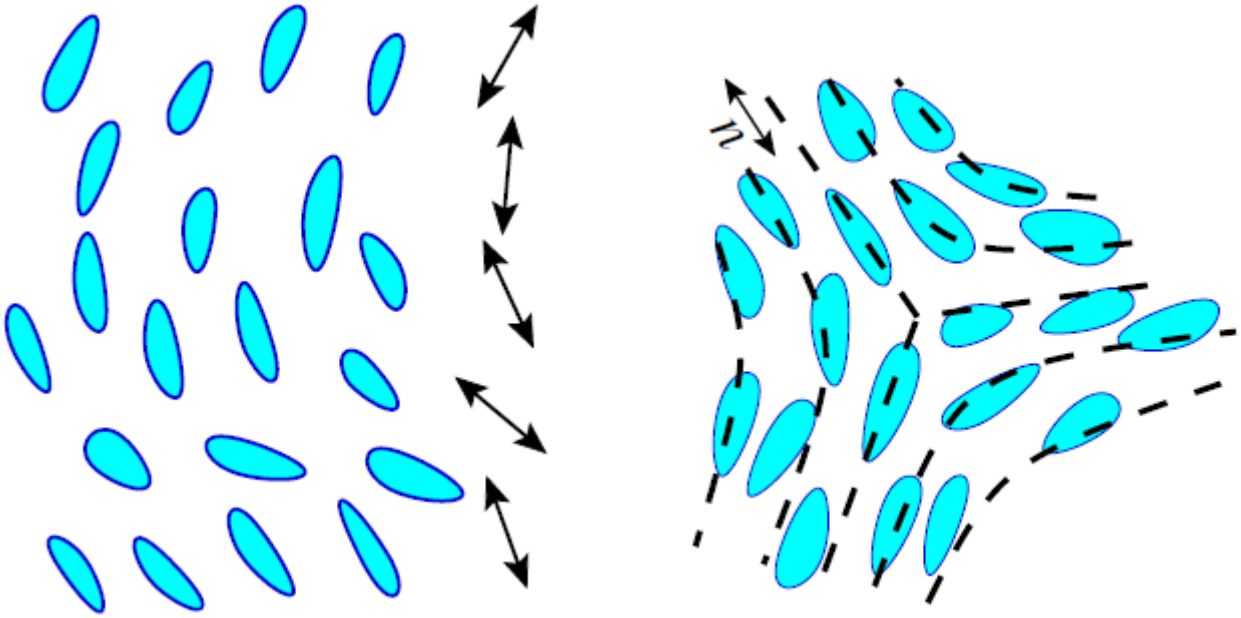

Figura 31: nematic; $\pi_1(\mathcal{RP}^2) = \mathcal{Z}_2$

disclinations with integral winding number (see fig.). They have the same rules for combining defects as the xy-model. The motopy group is that of integers under addition, that is,

$$\pi_1(P_1) = Z$$

We have a quite different situation for a three dimension space. We cannot have a topologically stable line defect for a three-component vector order parameter in three dimensions space as we already discussed. However, for the nematic, the order parameter space P_2 is the

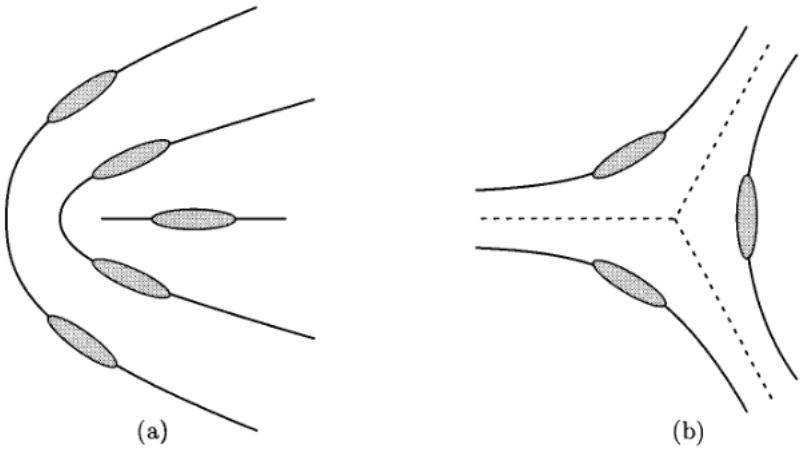

Figura 32: (a) $k = +1/2$ and $k = -1/2$ disclinations in a two-dimensional nematic. (CL)

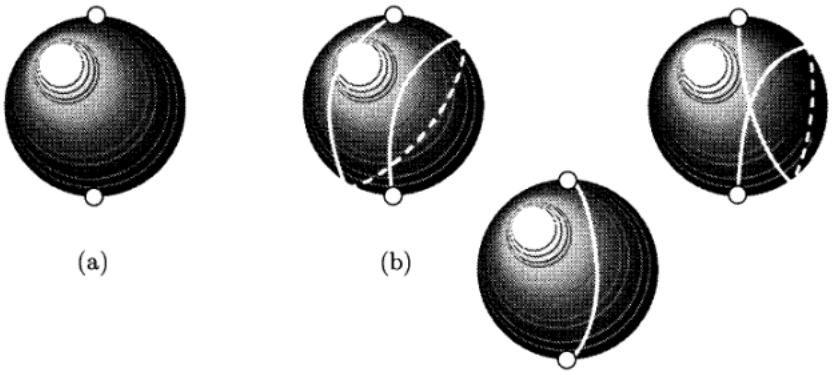

Figura 33: (a) Order parameter space, the surface of a sphere with antipodal points identified, for a three-dimensional nematic. (b) Distortion of a path with $k = 3/2$ to one with $k = 1/2$. (CL)

unit sphere $S_2$with antipodal points identified (or a projective space, $\mathcal{RP}^2$, half-hemisphere). We can therefore have a stable defect with a winding number of 1/2. In this case, we cannot deform to a point a path starting at one pole and ending at the other. Actually, all other half-integer paths can be deformed to the 1/2 path (see fig.).We have then only one stable line defect in a nematic liquid crystal. The homotopy group is simple the integers modulo 2, or,

$$\pi_1(P_2) = Z_2$$

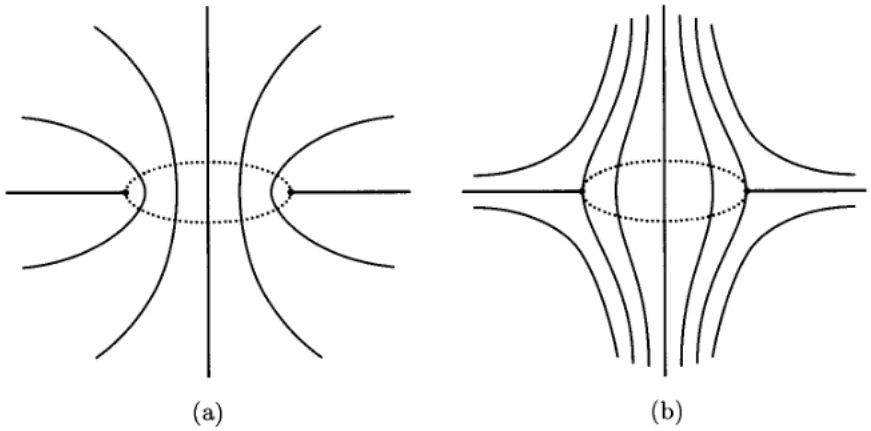

Figura 34: Disclination loops in a nematic formed by rotating about a vertical aixs the $k = 1/2$ and $k = -1/2$disclinations. The far fields correspond to the $+1$ hedgehog defect. (CL)

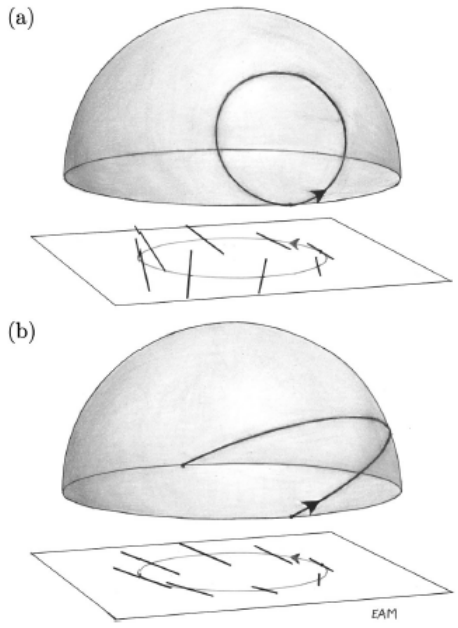

Figura 35: Three-dimensional netamic in theprojective plane $\mathcal{RP}$. (a) Trivial. (b) Nontrivial, $\pi_1(\mathcal{RP}^2) = Z_2$.

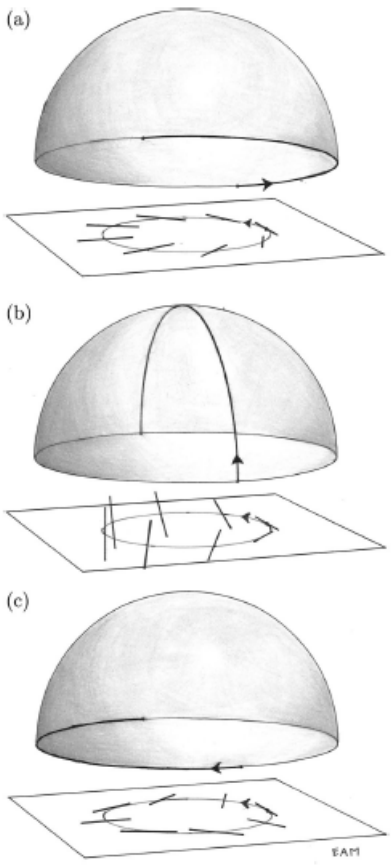

Figura 36: Homotopy taking $k = +1/2$ to $k = -1/2$.

7.5 Energy of vortices

We divide the energy E_v of the vortex in two parts: (1) the core energy E_c and (2) the elastic energy E_{el}.

The core energy is responsible for the destruction of the order parameter at the origin. Its calculation requires a microscopic description. We will limit ourselves here to a simple description. If we follow the Landau model, we now that the destruction of the order parameter is the condensation energy density f_{cond} of the ordered state. In the ϕ^4 model, it is simply

$$f_{cond} = \frac{r^2}{16u}$$

E_c is of order of the volume (or area) of the defect times f_{cond}. We have therefore for a vortex in two dimensions,

$$E_c \sim Aa^2 f_{cond}$$

where $A$is a numerical constant. The same expression is valid for the core energy per unit length of a vortex line in three dimensions.

Let us now consider the elastic energy. This is associated with the spatial variation of the order parameter or the elastic energy. For a vortex in two-dimensions, in the xy-model, with winding number, we have the constraint

$$\oint d\theta = 2k\pi$$

We have to minimize the elastic free energy

$$\frac{\delta F_{el}}{\delta \theta(\vec{r})} = -\rho_s \nabla^2 \theta(\vec{r}) = 0$$

subjected to the previous constraint. We observe that the field

$$\theta = k\phi$$

$$\vec{v}_s \equiv \vec{\nabla}\theta = \frac{k}{r}\hat{e}_\phi$$

with $r = (x^2 + y^2)$ and $\phi = \tan(y/x)$ satisfies the circuit constraint and the equilibrium condition everywhere except at the origin.

We can now calculate the elastic energy (or the free energy) for the vortex,

$$\begin{aligned} E_{el} &= \frac{1}{2}\rho_s \int d^2 r \vec{v}_s^2 = \frac{1}{2}\rho_s 2\pi k^2 \int_a^R \frac{rdr}{r^2} \\ &= \pi k^2 \rho_s \ln(R/a) \end{aligned}$$

Here, a is the core radius and R the linear dimension of the sample.

Finally, the total energy of the vortex is

$$E_v = E_{el} + E_c$$

We do not know the value of the core radius a.We can calculate it by minimizing E_c. The total energy is

$$E_v = Aa^2 f_{cond} + \pi k^2 \rho_s \ln(R/a)$$

and the minimization condition is

$$2Af_{cond} - \frac{\pi k^2 \rho_s}{a} = 0$$

which gives

$$a^2 = \frac{\pi k^2}{2} \frac{\rho_s}{A f_{cond}}$$

But, we know that

$$f \sim T_c \xi^{-d}$$

(eq. 5.4.17 CL)

and

$$\rho_s \sim t^{(d-2)\nu}$$

(eq. 6.1.11 CL, Josephson relation), but

$$\xi \sim |T - T_c|^{-\nu}$$

(eq. 5.4.3 CL), and we have

$$\rho_s \sim T_c^{(2-d)\nu} \xi^{2-d}$$

and, finally,

$$a^2 = \frac{\pi k^2}{2} \frac{\rho_s}{A f_{cond}} \sim k^2 \xi^2$$

The core length is proportional to k and to the correlation length, ξ. The core energy is then

$$E_c = \pi \rho_s k^2 / 2$$

Let us calculate following a different method. We know that $\vec{v}_s$ is a continuous variable whereas θ is multivalued. To handle that we introduce a cut in θ with a discontinuity of $2k\pi$. We lable the two surfaces by $\Sigma^+$and Σ^- and we have $\theta = 0$ on Σ^- and $\theta = 2k\pi$ on Σ^+. These two surfaces have the normal directions $-\hat{e}_\phi$and $+\hat{e}_\phi$, respectively. We can now integrate the elastic energy,

$$E_{el} = \frac{1}{2}\int d^2r\rho_s(\vec{\nabla}\theta)^2 = \frac{1}{2}\int \theta\vec{h}_s \cdot d\vec{\Sigma} - \frac{1}{2}\rho_s \int d^2r\theta\nabla^2\theta$$

where we introduced the field

$$\vec{h}_s = \rho_s\vec{v}_s$$

which is conjugate to $\vec{v}_s$. We have then

$$\begin{aligned} E_{el} &= \frac{1}{2}\left(\int \theta^+\vec{h}_s \cdot d\vec{\Sigma}^+ + \int \theta^-\vec{h}_s \cdot d\vec{\Sigma}^-\right) \\ &= \frac{1}{2}(\theta^+ - \theta^-)\int_a^R dr\rho_s\,|\vec{v}_s| \\ &= \pi k^2\rho_s \ln(R/a) \end{aligned}$$

We can calculate the interaction energy between two vortices. This is done by introducint a cut for each vortex (see fig.). First, we have to calculate the solution for the equation

$$\nabla^2\theta = 0$$

for vortices with strength k_i at the positions

$$\vec{r}_i = (x_i, y_i)$$

The solution is

$$\theta(\vec{r}) = \sum_i \theta_i$$

with

$$\theta_i = k_i \tan^{-1}[(y - y_i)/(x - x_i)]$$

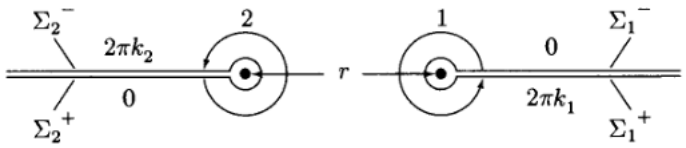

Figura 37: Cut for two non-intersecting vortices. (CL)

We can write now the elastic energy as

$$\begin{aligned} E_{el} &= \frac{1}{2}\int d^2r \rho_s (\vec{v}_s^{(1)} + \vec{v}_s^{(2)})^2 \\ &= E_1 + E_2 + \frac{1}{2}\int d^2r (\vec{h}_s^{(1)} \cdot \vec{v}_s^{(1)} + \vec{h}_s^{(2)} \cdot \vec{v}_x^{(2)}) \\ &= E_1 + E_2 + \frac{1}{2}(\theta_2^+ - \theta_2^-)\int_a^R dr \rho_s \frac{k_1}{r} + \frac{1}{2}(\theta_1^+ - \theta_1^-)\int_a^R dr \rho_s \frac{k_2}{r} \\ &= E_1 + E_2 + 2\pi\rho_s k_1 k_2 \ln(R/a) \end{aligned}$$

E_1 e E_2 are the energies of the isolated vortices, separated by r. Combining common terms, we have

$$E_{el} = \rho_s \pi (k_1 + k_2)^2 \ln(R/a) + 2\pi\rho_s k_1 k_2 \ln(a/r)$$

We observe that if $k_1 = -k_2$ the divergent term in R disappears. Actually, this happens whenever $\sum_\alpha k_\alpha = 0$. As a consequente, for $T > 0$, we can easily excite these configurations.

Also, the sign of the interaction energy depends on the relative sign of k_1 and k_2, being attractive whenever they have opposite signs.

The importance of this result is in the low value of the energy necessary to excite a vortex pair. Also, this value can be negative, therefore attractive. This plays a crucial role in the excitation and stability of vortices in the system.

7.6 Vortex unbinding, stiffness and Kosterlitz-Thouless transition

7.6.1 Vorticies and waves stiffness

We know now that the vortices are topologically stable. They are a topologically stable excitation of the ordered phase of the physical system with a continuous symmetry with the $U(1)$. (This can be extended to other topologically stable defects in other continuous symmetry systems). These excitations are different from the modes of Goldstone or, in our case, the spin-wave like excitations. In the spin-wave excitations, the phase of the superfluid velocity is longitudinal or proportional to the gradient of a scalar function. For the topological stable excitations, the order parameter amplitude disappears at the core. We have therefore an amplitude fluctuation and the average amplitude of the order parameter decreases. This leads to some consequences:

- a sufficiently large number of vortices can destroy the long range order;
- the proliferation of thermally activated vortices can lead to a phase transition to the high-temperature disordered phase;
- vortices reduce the (spin-)wave stiffness;
- vortices screen and reduce the energy of elastic distortions;
- thermally excited vortices in thermal equilibrium contribute with terms proportional to $e^{-E_c/T}$ (E_c is the core energy) to the partition function;
- this (above) term have essential singularities even at $T = 0\,K$.

Vortices are mobile degrees of freedom. The arrange themselves to minimize the free energy of any contribution originate from a macroscopic gradient of the phase of the order parameter (elastic energy). Let us consider our simple example, the xy-model. The vortices are in the phase $\theta(\vec{r})$ which has a uniform gradient. Let us consider a field ψ with phase $\vartheta(\vec{r})$ and where $<\psi>$ is the order parameter:

$$\psi = |\psi(\vec{r})|\, e^{i\vartheta(\vec{r})}$$

and

$$\theta(\vec{r}) =< \vartheta(\vec{r}) >$$

Let us consider the partition function for a $\theta(\vec{r})$ that is spatially uniform. For that, $\vartheta(\vec{r})$ may fluctuate but we impose a value of zero at the edges of the sample as boundary conditions. We have then

$$\frac{1}{\Omega}\int d^d r < \vec{\nabla}\vartheta(\vec{r}) >= \frac{1}{\Omega}\int d\vec{S} < \vartheta(\vec{r}) >= 0$$

where Ω is the volume of the sample. Let us now assume a spatially uniform gradient of θ, that is,

$$\vartheta(\vec{r}) = \vartheta'(\vec{r}) + \vec{v}\cdot\vec{r}$$

where $\vartheta'(\vec{r})$ is constrained to be zero on the boundaries. We can easily verify that

$$\vec{\nabla}\theta(\vec{r}) =< \vartheta(\vec{r}) >=< \vartheta'(\vec{r}) > +\vec{v}$$

and, therefore,

$$\vec{\nabla}\theta = \frac{1}{\Omega}\int d^d < \vec{\nabla}\vartheta(\vec{r}) >= \vec{v}$$

We find the macroscopic spin-wave stiffness renormalized by the fluctuations and vortices by calculating the difference in free energy between the system with $\vec{v} \neq 0$ and $\vec{v} = 0$:

$$F(\vec{v}) - F(0) = \frac{1}{2}\Omega\rho_s^R v^2$$

The xy-hamiltonian, at low temperatures, is a function of the velocity $\vec{v}_s = \vec{\nabla}\vartheta(\vec{r})$. We decompose the microscopic angle ϑ into an analytical part ϑ_a and a singular part ϑ_{sing}, the later arising from the vortices. The velocity is then the sum of a longitudinal part, $\vec{v}_s^{\shortparallel} = \vec{\nabla}\vartheta_a$ and a transverse par $\vec{v}_s^{\perp} = \vec{\nabla}\vartheta_{sing}$, where

$$\vec{v}_s = \vec{v}_s^{\shortparallel} + \vec{v}_s^{\perp}$$

with

$$\vec{\nabla} \times \vec{v}_s^{\shortparallel} = 0$$

$$\vec{\nabla} \cdot \vec{v}_s^{\perp} = 0$$

In the presence of a uniform average gradient, we have

$$\vec{v}_s = \vec{v} + \vec{v}_s^{\shortparallel} + \vec{v}_s^{\perp}$$

and $\vartheta_a(\vec{r})$ is zero on the boundaries so to assure that the spatial average of $\vec{v}_s^{\shortparallel}$ is zero for every configuration of the system.

We can now calculate the free energy of the system,

$$F(\vec{v}) = -k_B T \ln \mathrm{Tr} \exp[-\mathcal{H}(\vec{v})/k_B T]$$

where

$$\mathcal{H}(\vec{v}) = \frac{1}{2}\rho_s \int d^d r (\vec{v} + \vec{v}_s^{\shortparallel} + \vec{v}_s^{\perp})^2 + \mathcal{H}'$$

where ρ_s is the bare spin-wave stiffness unrenormalized by the vortices and $\mathcal{H}'$ is independent of $\vec{v}_s$ and $\mathcal{H}'$ is independent of $\vec{v}_s$ and we will drop it off. We have then

$$\begin{aligned} F(\vec{v}) &= \frac{1}{2}\Omega\rho_s v^2 \\ &= -k_B T \ln \mathrm{Tr} \exp[-\mathcal{H}(\vec{v}=0)/k_B T] \exp\left\{-(\rho_s/k_B T)\int d^d[\vec{v}\cdot\vec{v}_s(\vec{r})]\right\} \\ &= \frac{1}{2}\Omega\rho_s v^2 - \frac{1}{2}(\rho_s^2/k_B T)\int d^d r d^d r' \left\langle \vec{v}_{si}(\vec{r})\vec{v}_{sj}(\vec{r}')\right\rangle v_i v_j + F(0) + 0(v^4) \end{aligned}$$

We considered boundary conditions that imply a spatial average of $\vec{v}_s^{\shortparallel}$ for evryt configuration in the partition function trace. The longitudinal part does not give any contribution. We use now the limit

$$\lim_{\vec{q}\to 0} \vec{v}_s^{\shortparallel} \sim \delta_{ij} - \hat{q}_i \hat{q}_j$$

After a lengthy calculation we obtain

$$\rho_s^R = \rho_s - \frac{\rho_s^2}{(d-1)k_B T}\int d^e r \left\langle \vec{v}_s^{\perp}(\vec{r})\vec{v}_s^{\perp}(0)\right\rangle$$

The details are in the Chaikin-Lubensky, in particular in the Appendix 9A.

This is our main result: thermally excited vortices, responsible for a nonvanishing transverse part of $\vec{v}_s$, reduce the macrsocopi spin-wave stiffness ρ_s^R. This has its consequences in the dynamics of the order phase as well as the phase transitions conditions. We can express this result considering that the longitudinal and transversal part of $\vec{v}_s$ are decoupled in $\mathcal{H}$, or:

$$\vec{v}_s^{\shortparallel} \cdot \vec{v}_s^{\perp} = 0$$

Altso,

$$< \vec{v}_s^{\shortparallel}(\vec{q}) \cdot \vec{v}_s^{\shortparallel}(-\vec{q}) >= k_B T/\rho_s$$

and with

$$\vec{g}(\vec{r}) \equiv \rho_s \vec{v}_s(\vec{r})$$

we finally writhe

$$\rho_s^R = \frac{1}{k_B T} \int d^d r \left(< \vec{g}^{\shortparallel}(\vec{r}) \cdot \vec{g}^{\shortparallel}(0) > - \frac{1}{d-1} < \vec{g}^{\perp}(\vec{r}) \cdot \vec{g}^{\perp}(0) > \right)$$

7.6.2 Kosterlitz-Thouless transition

The history of phase transitions in two dimensions is quite long. Peierls (1935) was the first to present an argument against the existence of long-range order in a two-dimensional solid. He consider the thermal motion of long-waelength phonons which would destroy this order. The mean square deviation of an atom from its equilibrium positions increases logarithmically with the size of the system. As a consequence the Bragg peaks of the diffraction pattern broaden instead of being sharp, a characteristic of the crystalline order (note that this is a different effect than the Debye-Waller factor, which reduces the peaks but do not broaden

them). Mermin (1968) confirmed this result using rigorous inequalities. Mermin and Wagne (1966) demonstrated the abscence of the spontaneous magnetizaiton in a two-dimensional magnet with spins with mor than one degree of freedom. Hohenberg (1967) showed that the expectation value of the superfluid order parameter in a two-dimensional Bose fluid is zero. In our course, we found this result in several occasions. In particular, we observed that for the xy-model the order parameter correlation function dies off algebraically rather exponentially, indicating the possibility of a quasi-long-range order.

Several numerical works indicated, however, the existence of order. Alder and Wainwright (1962) observed a phase transition between a gas and solid phase in hard discs. Stanley and Kaplan (1966) observed the susceptibility of two-dimensional spin models go to infinite, an indication of phase transition. They performed a high-temperature series expansion calculation. It is important to emphasize that this observation is much stronger for the xy-model (Stanley (1968)) than for the Heisenberg model (Moore (1969)). Finally, Kosterlitz and Thouless, in a series of papers (ref.), argument in favor of the existend of a long-range order in some two-dimensional systems. This order, however, has a different nature than the one we discussed so far. Instead of being a consequence of the behaviour of the two-point correlation function, the orde is now an overall property of the system, a topological order. They observe this result for the two-dimensional solid, neutral superfluid and the xy-model. There is not such order for the superconductor or isotropic Heisenberg model. Berezinskii (1971) showed similar results.

We will not discuss this result in any detail, which would require the use of the renormalization group theory. CL give a detailed analysis for this transition. The analysis is on the existence of the vortices and they role in this topological order. Let us first recall some of the previous results for the xy-model (see Section 6.1 CL) calculated in the lattice model. The correlation function,

$$G(\vec{r},0) = \langle \psi(\vec{r}), \psi(0) \rangle = |\psi|\, e^{-g(\vec{r})}$$

where

$$
\begin{aligned}
g(\vec{r}) &= k_B T \int \frac{d^d q}{(2\pi)^d} \frac{1 - e^{i\vec{q}\cdot\vec{r}}}{\rho_s q^2} \\
&\quad \frac{k_B T K_d \Lambda^{(d-2)}}{(d-2)\rho_s} \quad |\vec{r}| \to \infty \ \ (d > 2) \\
&= \quad \frac{k_B T}{2\pi\rho_s} \ln(\tilde{\Lambda}\,|\vec{r}|) \quad |\vec{r}| \to \infty \ \ (d = 2) \\
&\quad \frac{k_B T}{2\rho_s} |x| \quad |x| \to \infty \ \ (d = 1)
\end{aligned}
$$

where $\tilde{\Lambda} = \Lambda e^{\tilde{\gamma}}$, Λ is a high wave number cutoff and $\tilde{\gamma} = \gamma + \frac{1}{2}\ln 8$, $\gamma = 0.5772$ (Euler-Mascheroni constant) for a square lattice model. Let us concentrate in the $d = 2$ case. We have here

$$G(\vec{r}, 0) = |\psi|^2 \, (\tilde{\Lambda}\,|\vec{r}|)^{-\eta}$$

where

$$\eta = \frac{k_B T}{2\pi\rho_s}$$

This behavior, a power-law decay of order-parameter correlation function, characterizes a quai-long-range order (QLRO). If T/ρ_s is neither zero nor infinite, the correlation function G$(\vec{r}, 0)$ shows a power-law dependence on $\vec{r}$ similar th a critical point in higher dimensions. In $q-$space,

$$G(\vec{q}) \sim |\vec{q}|^{-(2-\eta)}$$

as for a correlation function at a critical point. $G(\vec{q} = 0)$ as well as the uniform susceptibility is infinite for all $\eta < 2$. For $T = 0$ we have $g(\vec{r}) = 0$ and $G(\vec{r}, 0)$ is a constant independent of $\vec{r}$, indicating a long-range order in the two-dimensional classical xy-model at

zero temperature. Still, if we now consider the vortices effects on ρ_s, and we have $\rho_s \to 0$ with $T/\rho_s \to \infty$, then $G(\vec{r}, 0)$ will go to zero at large $|\vec{r}|$more rapidly than algebraically. This characterizes a transition from QLRO to disorder.

Let us examine this transition following a simple argument. We start with the calculation of the vortex energy which was discussed previously. For a unit strength vortex, in a sample with a linear dimension R, we have

$$E_v = \pi\rho_s \ln(R/a)$$

Since the core, with typical dimension a, can be anywhere in the sample, we can write the number or vortices as

$$N = (R/a)^2$$

and the entropy will be

$$S = k_B \ln N = 2k_B \ln(R/a)$$

The free energy for the xy-model with a single vortex is

$$F = E - TS = (\pi\rho_s - 2k_B T) \ln(R/a)$$

This simple result indicates that for $T < \pi\rho_s/2k_B$ the free energy minimizes in the absence of vortices. The opposite happens for $T > \pi\rho_s/2k_B$, when the presence of vortices is favored. The vortices destroy the phase ridid ity and we can identify a transition temperature

$$T_{KT} = \pi\rho_s/2k_B$$

as the temperature when first appears the vortices indicating a phase transition from

the algebraically order system to the disorder system. Actually, detailed calculations show similar result with ρ_s^R replacing ρ_s.

The net result is that for $T > T_{KT}$, vortices begin to proliferate. As a consequence, $G(\vec{r}, 0)$ begins to decay exponentially on a lenth scale given by the typical spacing between vortices,

$$G(\vec{r}, 0) \sim e^{-r/\xi(T)}$$

where $\xi(T)$ scales with the square root of the vortices density. From renormalization group theory, we obtain

$$\xi(T) \sim e^{-b|T-T_{KT}|^{-1/2}}$$

which is a divergence faster than any power law and the correlation length exponent defined by $\xi \sim |T - T_{KT}|^{-\nu}$ obeys $\nu = \infty$.

For lower temperatures, $T < T_{KT}$,vortices exist only in bound pairs with opposite vorticity. They are held together by a logarithmic confining potential.

Bound pairs of vortices at short distances) renormalize the bare spin stiffness ρ_s. Above T_{KT}, the finite density of unbound vortices causes the spin stiffness to drop discontinuously to zero. We observe a universal jump in the (e.g. superfluid) density.

Leitura recomendada:

(1) H.J. Jensen, The Kosterlitz-Thouless Transition (http://www.mit.edu/~levitov/8.334/notes/XYn

(2) S.M. Girvin, The Kosterlitz-Thouless Phase Transition (http://zimp.zju.edu.cn/~tcmp/refpdf/KT Girvin.pdf)

Referências

[1] James P. Sethna, **Entropy, Order Parameters, and Complexity**, Oxford Master Series, Oxford University Press, 2006; ver também a página do autor http://www.lassp.cornell.edu/sethna/

[2] P.M. Chaikin e T.C. Lubensky, **Principles of condensed matter physics**, Cambridge University Press, 1995.

[3] Sílvio R. A. Salinas, **Introdução à Física Estatística**, EdUSP, 1997.

[4] David Chandler, **Introduction to Modern Statistical Mechanics**, Oxford University Press, 1987.

[5] Harvey Gould e Jan Tobochnik, **Statistical and Thermal Physics**, Princeton University Press, 2010 e http://www.compadre.org/stp (Statistical and Thermodynamic Project, apoiado pela National Science Foundations – EUA).

[6] Edouard Brézin, **Introduction to Statistical Field Theory**, Cambridge University Press, 2010.

[7] R.M. White, **Quantum Theory of Magnetism**, Springer, 1970.

[8] A. Zunger, L.G. Wang, G.L.W. Hart, e M. Sanatai, "Obtaining Ising-like expansions for binary alloys from firstt principles", em *Modelling and Simulation in Materials Science and Engineering*, **10**, 685 (2002).

[9] H. Gould e J. Tobochnik e W. Christian, **An Introduction to Computer Simulation Methods**, 3a. ed., pp. 646-649, Addison-Wesley (2006)

[10] M.P. Marder, **Condensed Matter Physics,** 2a. ed., Wiley-Interscience, 2010.

[11] K.J. Wilson e J. Kogut, "The Renormalization Group and the ϵ-expansion", *Physics Reports **12**,* 75 (1974).

[12] G. Parisi, **Statistical Field Theory**, Addison-Wesley Publ. Company, 1988.

[13] C. Domb e A.J. Guttmann, "Low-temperature series for the Ising model", *J. Phys. C: Solid St. Phys.,* **3**, 1652 (1970).

[14] N.D. Mermin, *Rev. Mod. Phys.* **51**, 591 (1976).